DE GRUYTER Nanophotonics 2021; 10(16): 3945–3955

Review

Wanxiao Gao, Jie Ding*, Zhenxu Bai, Yaoyao Qi, Yulei Wang and Zhiwei Lv

Multiple excitons dynamics of lead halide perovskite

https://doi.org/10.1515/nanoph-2021-0411
Received July 28, 2021; accepted October 10, 2021;

Abstract: The lead halide perovskite material shows its unique photoelectric properties, the resulting conversion efficiency of perovskite solar cells. However, the efficiency comes to a bottleneck owing to that mechanism research fall behind the device research. Multiple excitons dynamics play an important role， especially in the lifetime and binding energy of multiple excitons. A long multiexciton lifetime is beneficial to the application for light-emitting devices and photovoltaic devices. Large multiexciton binding energy means a large Stokes shift in exciton absorption, thus avoiding the loss of linear absorption. To conclude, discussions are presented regarding views of current multiple excitons research in terms of the biexciton lifetime and biexciton binding energy that should be considered for further advances in materials and devices.

Keywords: biexciton binding energy; biexciton lifetime; lead halide perovskite; multiple excitons.

1 Introduction

Lead halide perovskite materials with high quantum efficiency [1], high carrier mobility [2], electronic band gap adjustable [3], and simple solution processing have attracted much attention [4–8]. The extraordinary performance in optoelectronic devices such as solar cells [9], photodetectors [10], and lasers [11–13] makes it one of the most promising emerging materials [7, 16–18]. After the blowout study of perovskite solar cells since 2009 [1, 17], the conversion efficiency of lead halide perovskite gradually slows down and approaches its theoretical limit [18]. The underlying study of the carrier transport mechanism is far behind device efficiency research. To reveal the fundamental issue, the exciton dynamics of perovskite need to be figured out [2].

In light-emitting technology, such as the light-emitting diode (LED) of the display, the emission color purity is very important. Under the device-related conditions, nanocrystalline may maintain multiple excitations at the same time, leading to the multiexciton state. Even when the single exciton dominates the device, Poisson absorption statistics will also lead to a few numbers of multiple excitons [14]. Nanocrystals can provide some additional beneficial properties. Due to quantum confinement, they can change the electrical and optical properties. One of the induced effects of quantum confinement is the increase of Auger recombination rate. The auger time constant is usually tens to hundreds of picoseconds, which depends on the multiplicity of excitons and the size and shape of nanocrystals. Auger recombination of multiple excitons sets an upper limit for the number of photons emitted. The study of the lifetime of multiple excitons is very important for the application potential of perovskite nanocomposites [17–19]. Compared with neutral excitons, multiple excitons show a very short lifetime [20]. Material properties can be modified through interfaces, modified device architectures, and physical constraints on the size of photoactive materials [21–23]. One such process utilized by physical constraints of light-absorbing materials is the multiple exciton generation process [24]. It is necessary to study the bulk excitons. Perovskite materials can exhibit a variety of exciton species, including biexciton and triple exciton [25], the dynamics process of these multiple excitons play an important role in understanding the multibody effect of lead halide perovskite, the power conversion efficiency of photovoltaic devices can also be improved by the

---

***Corresponding author: Jie Ding**, Center for Advanced Laser Technology, Hebei University of Technology, and Hebei Key Laboratory of Advanced Laser Technology and Equipment, Tianjin 300401, China, E-mail: dingjie@hebut.edu.cn. https://orcid.org/0000-0001-8343-8531
Wanxiao Gao, Yaoyao Qi, Yulei Wang and Zhiwei Lv, Center for Advanced Laser Technology, Hebei University of Technology, and Hebei Key Laboratory of Advanced Laser Technology and Equipment, Tianjin 300401, China
Zhenxu Bai, Center for Advanced Laser Technology, Hebei University of Technology, and Hebei Key Laboratory of Advanced Laser Technology and Equipment, Tianjin 300401, China; and MQ Photonics Research Centre, Department of Physics and Astronomy, Macquarie University, Macquarie Park 2109, NSW, Australia

multiexciton generation process. The conditions for the emergence of multiple excitons are not harsh. If the lifetime of multiple excitons is short, it means that the multiple exciton binding energy is low, the multiple excitons are unstable, which is not conducive to the application of lead halide perovskite materials.

2 Study of multiple excitons

Excitons and exciton complexes are produced by perovskite nanomaterials under different excitation conditions. The generation, separation, and recombination of exciton play a crucial role in the photophysical properties. Photoelectric properties of lead halide perovskite devices are determined by the exciton and exciton complexes [26]. When an electron is excited from the valence band to the conduction band, it creates a hole in the valence band and an electron in the conduction band. The generated electron–hole pair calls exciton [27]. Firstly, Wang et al. illustrated the dynamics of excited absorption PA2 and bleaching band PB1 in the $CH_3NH_3PbBr_3$ absorption spectrum, as shown in Figure 1a and b. It turned out that the bleaching band PB1 from photogenerated exciton, exciton and carrier can coexist, but excitons do not dominate and the exciton contribution is small [28]. However, after testing the $MAPbI_3$ with low binding energy [29, 30], Fang et al. measured the nanocrystals and thin films of $FAPbI_3$, as shown in Figure 1c and d. The trends of PL intensity of $FAPbI_3$ nanocrystals and $FAPbI_3$ polycrystalline thin film are inverse under higher excitation. In the nanocrystals, the luminous intensity increases linearly with the increase of pump energy. Under higher excitation, the slope becomes sub-linear. The change of slope is attributed to the interaction between excitons, and the biexciton recombination occurs under high pump energy. In the polycrystalline thin film, the PL intensity is quadratically dependent on the pump fluence for excitation above $6390\ nJ/cm^{-2}$. Therefore, the nongeminate bimolecular free electron–hole recombination becomes a dominant process at this excitation level. The free electron–hole recombination of the film in Figure 1d is the main process, so the exciton is an important particle in the nanocrystals [31]. Several studies have also shown that initially formed excitons rapidly dissociate into free carriers at ps time scales [32, 33], the dynamics observed on the time scale of ps is mainly exciton behavior production [28, 34, 35], tribromide perovskite also has excitons at room temperature [36]. Jiang et al. found that the exciton dominates the charge occupation and composite properties of the $MAPbBr_3$ at room temperature [37]. There are also reports that photogenerated excitons do not dissociate effectively without excess energy at the excitation wavelength, indicating that thermally activated excitons control the carrier dynamics of lead halide perovskite materials [34]. Light-emitting devices benefit from the ultrafast transfer of the excitons and the light-harvesting devices benefit from efficient exciton dissociation [38, 39], advances in optoelectronic devices depend on the understanding of exciton action [40]. Thus, the exciton kinetics of the perovskite material is crucial to better performance [41].

The multiexciton interaction enhances as the material scale of the lead halide perovskite material decreases [42]. The energy of the photon is higher than the bandgap, resulting in hot carriers, which cool to the band edge by releasing excess energy as waste heat. The excess energy produces one or more additional band-edge excitons larger than the band-gap of quantum dots, these are called multiple excitons. Biexcitons, trions, and other multiexcitons are also called multiple excitons. Perovskite nanomaterials can produce multiple excitons under strong excitation conditions. The simplest multiple excitons are biexciton, that is, four particles with two electrons and two holes are combined together. There is also a kind of multiple excitons in perovskite nanomaterials, which is called charged exciton, that is, trion. A trion is a combination of three particles, one electron (hole) and two holes (electron). The surface defect of perovskite nanocrystals is the root of producing charged excitons source. Under weak light excitation, perovskite nanomaterials mainly show single exciton recombination. At medium excitation intensity, perovskite nanomaterials mainly show biexciton recombination. Under strong light excitation, Auger recombination dominates the generation of charged excitons, and perovskite nanomaterials are mainly characterized by charged exciton recombination. This multiexciton generated by the absorption of a high-energy photon is called multiple exciton generation [16, 43]. The situation of charged excitons in perovskite devices is different. Due to the inherent asymmetry between the effective mass and mobility of electrons and holes, as well as the specific device architecture design when preparing devices, there is an imbalance between the injection and extraction rates of electrons and holes, which is easy to lead to the generation of charged excitons. For example, in LED devices, electrons are usually injected into perovskite nanocrystals at a faster rate than holes, resulting in negatively charged excitons. In solar cells, electrons are usually extracted from perovskite nanocrystals at a faster rate than holes, resulting in positively charged excitons. The interaction between excitons in perovskite nanocrystals is not repulsive but attractive [44]. It can improve the photo-current of photovoltaic

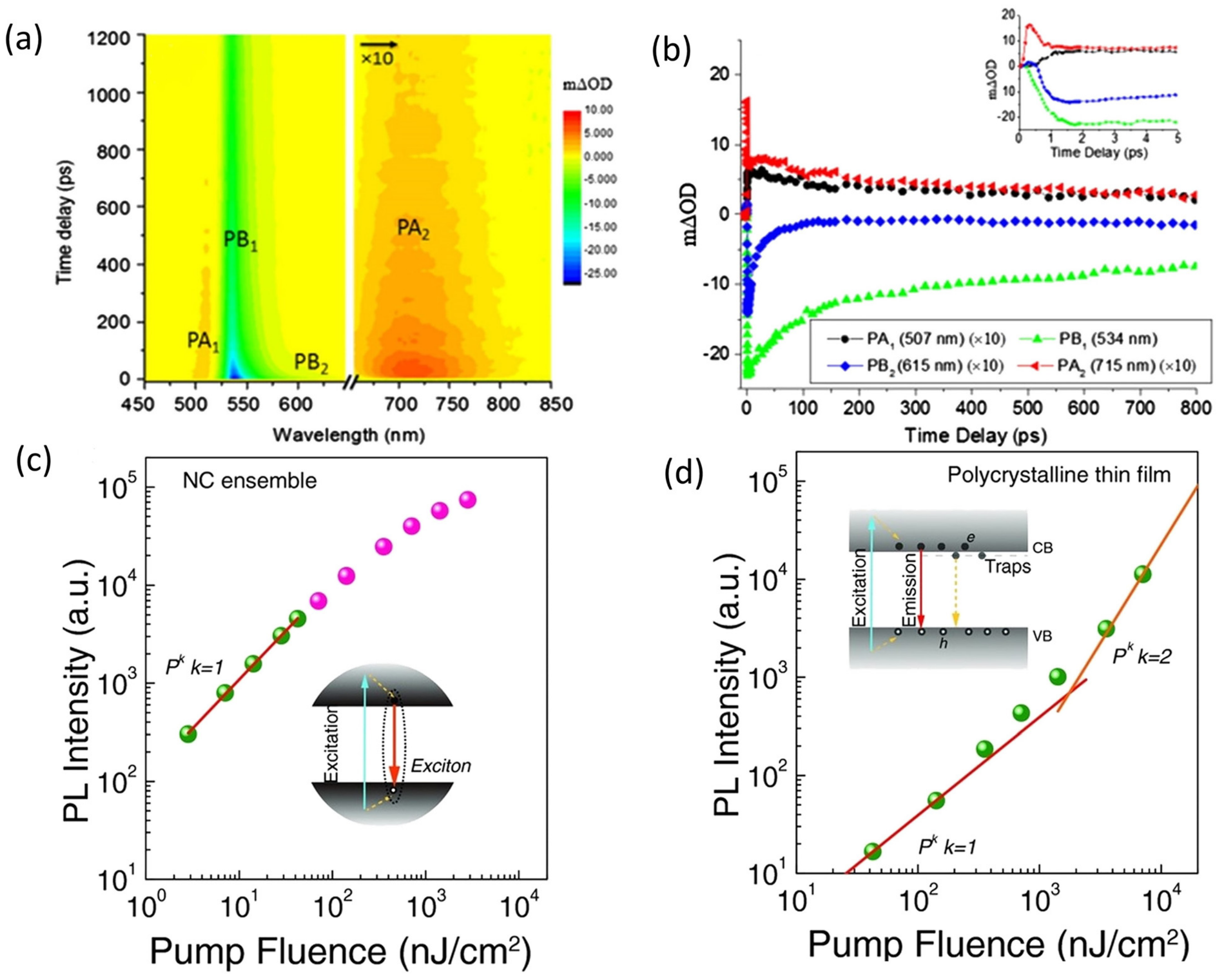

Figure 1: (a) $CH_3NH_3PbBr_3$ transient absorption (TA) spectra [28] (b) dynamics locus [28] (c) $FAPbI_3$ nanocrystals [31] (d) $FAPbI_3$ polycrystalline thin film [31].

devices and thus overcome the Shockley–Queisser limit [45]. Li et al. verified that the TA spectrum dynamics of multiple excitons with a lifetime of tens to hundreds of ps at low and high pump energy densities are the characteristics of multiple excitons, as shown in Figure 2a and b. The band-edge photobleaching dynamics exhibit a single exponential decay, indicating that there is no decay from the triplet exciton. The apparent rapid decay component of the amplitude increase appears (Figure 2a), the fast biexciton decay with a lifetime of about 160 ps persists at very low pump energies. This phenomenon of rapid biexciton decay at low pumping energies provided the first evidence for multiple excitons generation [46]. The study of multiple exciton interaction in perovskite nanocrystals provides a powerful tool to explore its application prospects in solar cells [47].

The process of multiexciton generation can observe in perovskite nanocrystals with slow hot carrier cooling. The dynamic process of $CsPbI_3$ is measured by Weerd et al. The TA spectroscopy proved that the ratio (A/B) between initial amplitude A and tail amplitude B remained unchanged at different pump energies (Figure 3a and b), excluding multiphoton absorption. Therefore, the observed increase in injection volume within this range only produces a higher number of stimulated nanocrystals. The dynamics around the ground state bleaching and the maximum absorption of the excited state were demonstrated by Weerd et al. as shown in Figure 3c, efficient (up to 98%) multiexciton generation was observed [48, 49]. The highly efficient multiexciton generation of perovskite may lead to the realization of next-generation solar cells [50].

Aneesh et al. found that when the average number of excitons in each nanocrystal is greater than 1, $CsPbBr_3$ nanocrystals have strong light–matter coupling and Coulomb interaction. It provides new insight to explore controlled multiple interactions in $CsPbBr_3$ nanocrystals: biexciton Stark effect produced by excitons generated by

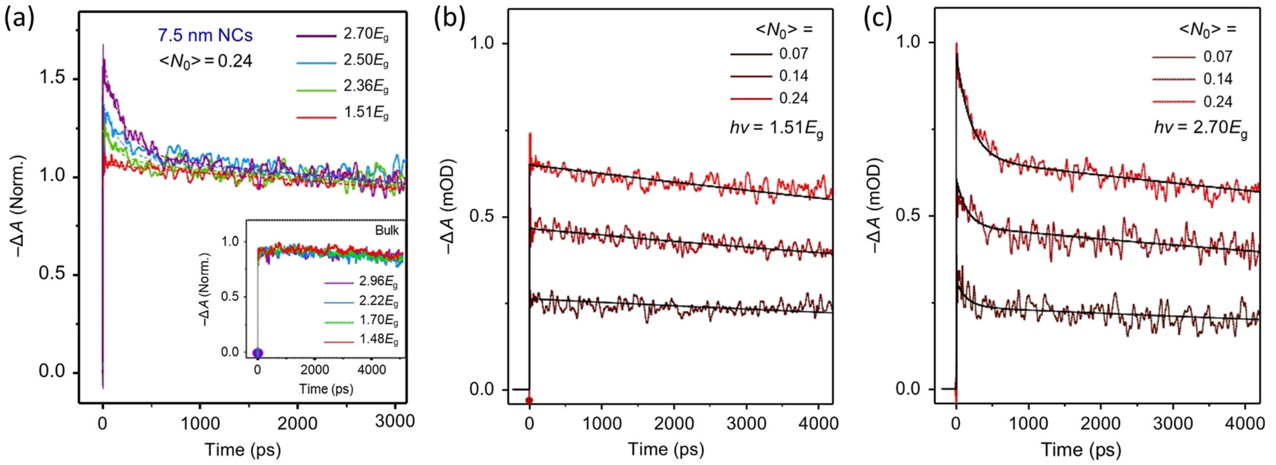

Figure 2: (a) Band-side bleaching kinetics at different pump photon energies in $FAPbI_3$ nanocrystals. The illustration shows the bulk sample measurements. TA dynamics at the pump energies of (b) 1.51 Eg and (c) 2.70 Eg. The solid black line is a single exponent in (b) and a double exponential fitting in (c), respectively [46].

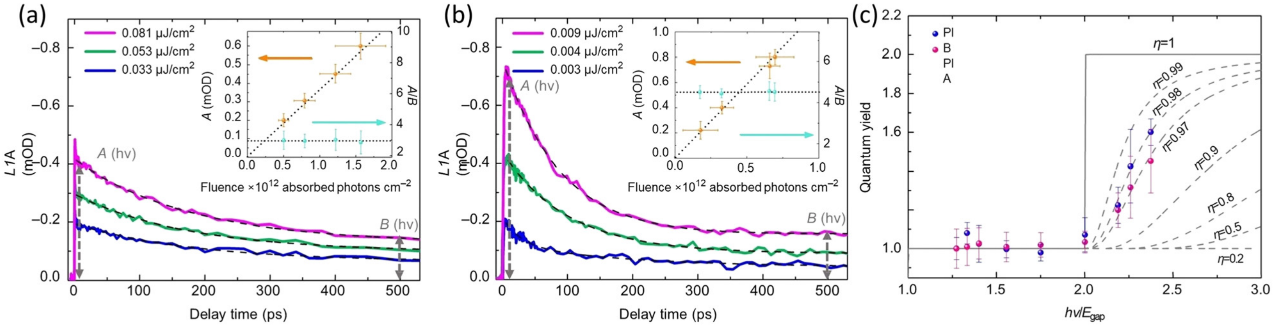

Figure 3: The dynamics of TA are lower than (a) and higher than (b) carrier multiplication threshold, and the dotted line represents the exponential fitting of the data. The illustration shows the *A*/*B* ratio. (c) The multiple exciton production efficiencies are plotted as a function of the excitation energy [48].

the pump and probe beams. It can be seen from the TA spectrum in Figure 4a that the redshift of the early exciton transition is consistent with the interaction between the excitons produced by the pump and probe beams, that is, the Stark effect caused by the Coulomb interaction of the biexcitons. It can be seen from Figure 4 that the magnitude of the redshift is independent of the pump beam injection amount, and it is due to the multiple exciton interaction produced by the probe beam [47, 51]. Perovskite can show multiple exciton products, including biexciton [52]. Biexciton dynamics is an important part of the carrier dynamics, especially the biexciton lifetime and biexciton binding energy. Some studies have shown that the formation of biexcitons can be greatly enhanced at higher excitation [53]. It also causes the multiple excitons nonradiative Auger recombination, which leads to the decrease of the lifetime of the biexciton. The fast relaxation of multiple excitons brings great complexity to the application of solar cells; hence the study of biexciton lifetime is particularly important [47]. On the other hand, the temperature dependence of the binding energy of the biexciton is that the dynamic disorder becomes an extremely relevant parameter in the multiple correlations, and the binding energy of the biexciton is lower than that of the single exciton, this makes the binding energy of biexciton more sensitive to the dynamic disorder caused by local lattice fluctuation. The size of the biexciton binding energy also affects the biexciton lifetime. In nanocrystals, due to quantum constraints, the radius of the biexciton will be reduced, the biexciton binding energy will be increased, and the biexciton lifetime will be increased. It is necessary to study the lifetime and binding energy of the biexc iton [54].

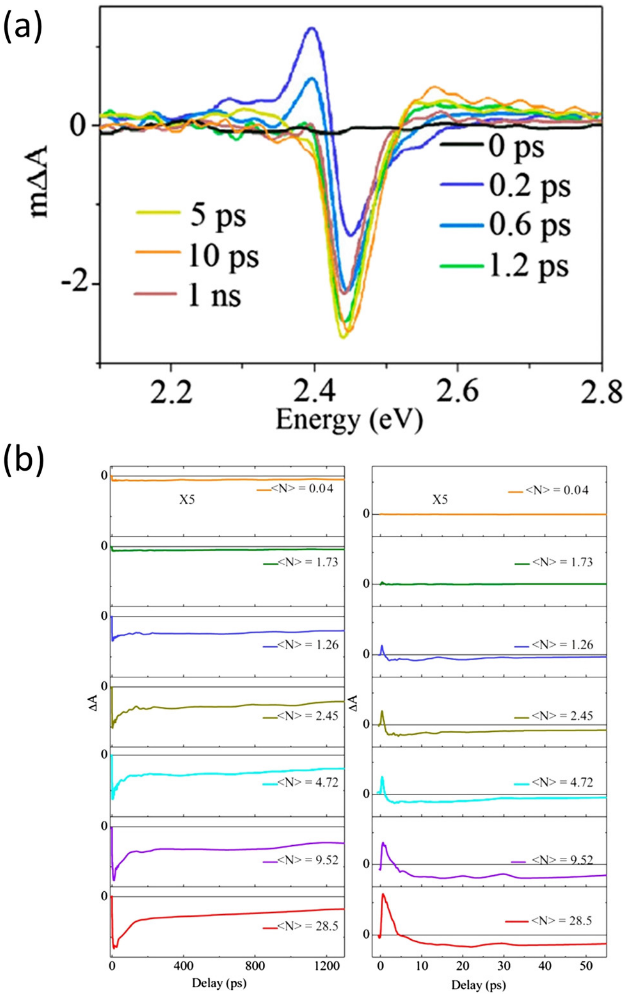

Figure 4: (a) TA spectrum of $CsPbBr_3$ at different delay times $CsbBr_3$ (b) bleaching signal (c) absorption signal of $CsPbBr_3$ nano-crystals under different pump injections [47].

3 Biexciton lifetime

A biexciton makes up of two excitons [55]. The biexciton lifetime is the time when the biexciton disappears through Auger recombination. At room temperature, the lifetime of biexciton is much shorter than that of the exciton. It is estimated that the lifetime of biexciton is half of that of the exciton. The short biexciton lifetime is not good for the application of lead halide perovskite materials in devices. The biexciton lifetime depends on material volume, pumping energy, and doping. Generally speaking, the interaction between its formation and dispersion controlled the decay time of biexciton [52]. Compared with the extraction time of the carrier, the lifetime of biexciton is also shorter. The study of multiple exciton lifetime is very important for the application of perovskite materials [19].

The stimulated emission mechanism in lead halide perovskite has been proved to come from the biexciton recombination, and the binding energy of the biexciton is 50 meV, which is better than the electron–hole recombination [56]. Mondal et al. found that doping a small amount of chloride can improve the biexciton lifetime of lead halide perovskite by slowing down the Auger recombination process so that the electrons can transfer quickly and obtained the doped perovskite with higher energy conversion efficiency [57]. It is found that the biexciton lifetime is related to the volume of perovskite nanocrystals, which is a common trend in other colloidal nanocrystals far higher than the band edge excitation [58]. As shown in Table 1, the biexciton lifetime of different samples is discussed. Generally, nanocrystals with different compositions exhibit similar biexciton lifetimes, which depend on the volume of nanocrystals. However, Makarov found that all inorganic cesium lead halide perovskite nanocomposites deviate from the general trend. It was observed that the volume of nanocrystals changes in a sub-linear manner, and the biexciton lifetimes are significantly shorter than previously reported (5–10 times) [59]. It can be seen from Table 1 that doping chlorine in the sample can significantly improve the biexciton lifetime by slowing down the Auger recombination process. The inhibition of Auger recombination rate and the extension of biexciton lifetime make these species be utilized through rapid electron transfer. The lifetime of 85 ps obtained by DeJong is two times longer than that of the same size nanocrystals (38–47 ps). DeJong et al. measured the dynamics of 8.6 nm $CsPbBr_3$ at different excitation pump energy densities. By fitting the lowest excitation pump energy flow transient to a single exponential function, the biexciton lifetime (Figure 5a) was about 85 ps. Based on the dynamic difference between the biexciton curve and the maximum excitation energy flow curve, the effective multi exciton

Table 1: Biexciton lifetime of different samples.

Samples	Size	Biexciton lifetime	Reference
$CsPbBr_3$	7 nm	44 ps	[61]
$CsPbBr_3$	7.7 nm	40 ps	[26]
$CsPbBr_3$	8.1 nm	38 ps	[59]
$CsPbBr_3$	8.6 nm	85 ps	[19]
$CsPbBr_3$	8.6 + nm	85 + ps	[56]
$CsPbBr_3$	9.3 nm	47 ps	[59]
$CsPbI_3$	–	115 ps	[57]
$FA_xCs_{1-x}PbI_3$	–	101 ps	[57]
$CsPbI_{3-y}Cl_y$	–	197 ps	[57]
$FA_xCs_{1-x}PbI_{3-y}Cl_y$	–	204.6 ps	[57]
$FAPbI_3$	–	145 ps	[57]

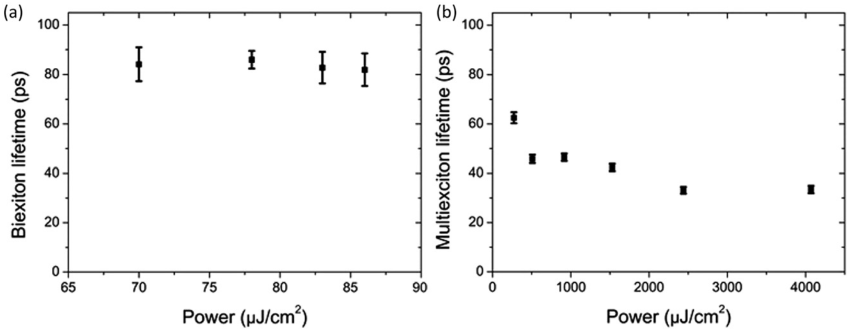

Figure 5: (a) The biexciton lifetime, after subtracting the contribution of a single excited nanocrystalline to the single exponential function, is obtained by fitting the lowest excitation pump flow. (b) After subtracting the contribution of a single excited nanocrystal line to the single exponential function, the multiexciton lifetime is determined by fitting the dynamics obtained for the highest excitation pump flow [19].

lifetime is estimated, which ranges from about 35 to 70 ps (Figure 5b) [19]. In DeJong's study, the contribution of multiple excitons was observed, and the lifetime of multiple excitons decreased significantly with the increase of pump injection (Figure 5b). The relatively short lifetime of the biexciton and multi exciton is not conducive to the application in light-emitting devices and photovoltaic devices, so it is necessary to suppress Auger recombination [19, 60]. Castaneda et al. have studied the multiple exciton interactions in a series of quantum dots $CsPbBr_3$ and $CsPbI_3$ samples, which were consistent with Makarov's work. Biexcitons are more likely to appear at high pump energies, but the life of biexcitons at high pump energies is shorter; proper doping can increase the biexciton lifetime. For $CsPbBr_3$ quantum dots whose size exceeds Bohr exciton radius, the biexciton interaction is sub-linear with the volume; for smaller quantum dot samples, the Auger lifetime of biexciton follows the same volume scale as other quantum dots. For larger quantum dots, Auger recombination has a strong dependence on composition. However, in addition to the limitation of composition, the binding energy of biexciton can prove the strong multiexciton interaction in quantum dots [15].

4 Biexciton binding energy

In perovskite nanomaterials, the binding energy of excitons directly affects the composite luminescence mechanism. The binding energy of excitons is related to material thickness and halogen octahedron. When the high flux light irradiates perovskite nanomaterials at room temperature, there are two mechanisms: exciton recombination luminescence and carrier recombination luminescence. Exciton composite luminescence and carrier composite luminescence are closely related to the size of the perovskite nanomaterials. With the increase of exciton binding energy in small-size nanocrystals, the photoluminescence emission can attribute to exciton recombination rather than free carrier bimolecular recombination [74]. Perovskite nanomaterials have high photoluminescence quantum efficiency, mainly because nanomaterials can enhance the exciton binding energy in perovskite materials, and ensure that the recombination in perovskite is dominated by free exciton emission. At the same time, nanomaterials can concentrate carriers in small sizes, which can significantly improve the carrier density [62]. The binding energy of exciton is affected by organic cation and quantum confinement effect. In all inorganic perovskite $CsPbBr_3$ nanocrystals, the exciton binding energy was 40 meV, and the Bohr radius of the exciton was 7 nm [63]. The excitons in organic–inorganic hybrid perovskite $MAPbBr_3$ and $FAPbBr_3$ nanocrystals have smaller binding energy and exciton radius [64, 65]. The quantum confinement potential will squeeze the electron–hole pair closer to the hole, so the exciton radius will be smaller. As the distance between the electron and the hole decreases, the Coulomb interaction increases, so the binding energy of the exciton increases, and the lifetime of the exciton increases. Large exciton binding energy and oscillator strength also lead to strong photoluminescence, nonlinear optical effect, and tunable polarization absorption [75]. The exciton binding energy of all inorganic perovskite $CsPbBr_3$ nanocrystals increases from 40 to 120 meV under quantum confinement [66]. At the same time, the exciton binding energy of perovskite nanomaterials is also affected by the morphology and quality of perovskite nanomaterials. The exciton binding energy in thin perovskite is only 41.4 meV, and that of cubic perovskite can reach 106.7 meV [67]. Using organic components with a high dielectric constant in two-dimensional (2D) perovskite can obtain very low exciton

Table 2: Exciton binding energies of halogen ions with different layers [65, 66].

Layer number (n)	X = Br (meV)	X = I (meV)
$n = 1$	752.3	498.1
$n = 2$	345.9	291.0
$n = 3$	218.5	195.6
$n = 4$	161.0	143.4
$n = 5$	129.9	111.5
$n = 6$	111.0	90.4
$n = 10$	79.8	50.7
$n = \infty$ (>100)	65.0	16.0

binding energy [68]. Iodine-based 2D perovskite shows about 320 meV exciton binding energy [76], and quasi 2D perovskite bridges the 2D and three-dimensional values [77, 78]. The exciton binding energy in the 2D perovskite nanomaterials strongly depends on the thickness of the material. The exciton binding energy of 2D perovskite $(C_6H_{13}NH_3)_2(CH_3NH_3)_{n-1}Pb_nI_{3n+1}$ with different thicknesses can increase from 100 to 361 meV [69]. Exciton binding energy will also be affected by the octahedral layers of perovskite and halogen ions, as shown in Table 2 below [70]. The large exciton binding energy affects the luminescence efficiency of materials and increases the exciton lifetime, which is more conducive to the application of lead halide perovskite materials in luminescent materials [71].

Large exciton binding energy is conducive to the application of materials. Similarly, in order to obtain high-performance devices, the biexciton binding energy should also be large to distinguish between excitons and biexcitons. Compared with two isolated single excitons, the multiple interactions can lead to the energy transfer of the biexcitons, which is mainly the result of the multiple Coulomb interactions [72]. The difference between the energy of the biexcitons and that of the double excitons is called the binding energy of the biexcitons, which may be attractive or repulsive. The binding energy of the biexcitons depends heavily on quantum constraints [1]. For laser applications, the energy of each multi exciton state determines which transition can maintain the population inversion. In recent years, many studies indicate the ultrafast process of a biexciton in large cubic nanocrystals. The existence of exciton can activate the bandgap transition in perovskite quantum dots with a strong confinement region, and emit laser in the process of biexciton exciton to exciton transition, so the biexciton binding energy is very important [16]. Yakunin pointed out that the large biexciton binding energy observed in quantum dots is expected to reduce the threshold of stimulated emission [6], and the high biexciton binding energy can evaluate the stability of biexcitons [60]. On the other hand, the smaller the binding energy of the biexciton makes it impossible to distinguish between the biexciton and the exciton contribution in the process of excitation and detection. Therefore, to study the relaxation dynamics of the biexciton in detail, the larger binding energy of the biexciton is needed [73]. The very large binding energy of biexcitons has been reported in both $CsPbBr_3$ and $CsPbI_3$ nanocrystals. For thermal excitons with larger excess energy, the binding energy of the biexcitons will become larger [74]. Castumeric et al. summarized the biexciton binding energies of several sizes, as shown in Figure 6a. The biexciton binding energies of quantum dot samples $CsPbBr_3$ and $CsPbI_3$ decrease with the increase of cross-section. In the weak confinement region, the two largest quantum dots have similar biexciton binding energies of 40 meV, which is close to the exciton binding energies of $CsPbBr_3$ measured in the weak confinement region, but still larger than that of bulk $CsPbBr_3$ (less than 10 meV). The biexciton binding energy of iodide quantum dots measured in the weak confinement region is 23 meV, which is close to the expected value. As shown in Figure 6a, the maximum binding energy of the biexciton can achieve at a similar size [15]. The large binding energy of biexciton has the same origin as an exciton. The large binding energy of biexciton means the large stoke displacement in exciton absorption, thus avoiding the linear absorption loss [52]. According to the method proposed by Aneesh et al. Li et al. [47] obtained similar biexciton binding energies for perovskite materials with different compositions by Gaussian function fitting, indicating that the material composition has little effect on the biexciton binding energies [1, 15, 47, 75]. Fang et al. observed that the biexciton binding energy of $(PEA)_2PbI_4$ is 45 meV at room temperature. Such a high biexciton binding energy makes these materials suitable for laser applications [52]. According to the report of Makarov et al., because the band edge of the two excitons is degenerate [59], the biexcitons must occupy the spin pairing state to eliminate the exchange contribution, so the Coulomb interaction is the main contribution to the binding energy of the biexcitons [16]. Yumoto et al. proposed that the binding energy of biexcitons is related to excess energy. As shown in Figure 6b, the binding energy of biexcitons increases monotonously with the increase of excess energy. This dependence also reflects that the thermal biexcitons with larger excess energy need to relax to the edge of the energy band for a long time, and the interaction between excitons and excitons will be stronger [74]. The presence of excitons can activate a forbidden transition in strongly confined perovskite quantum dots and the Stark effect

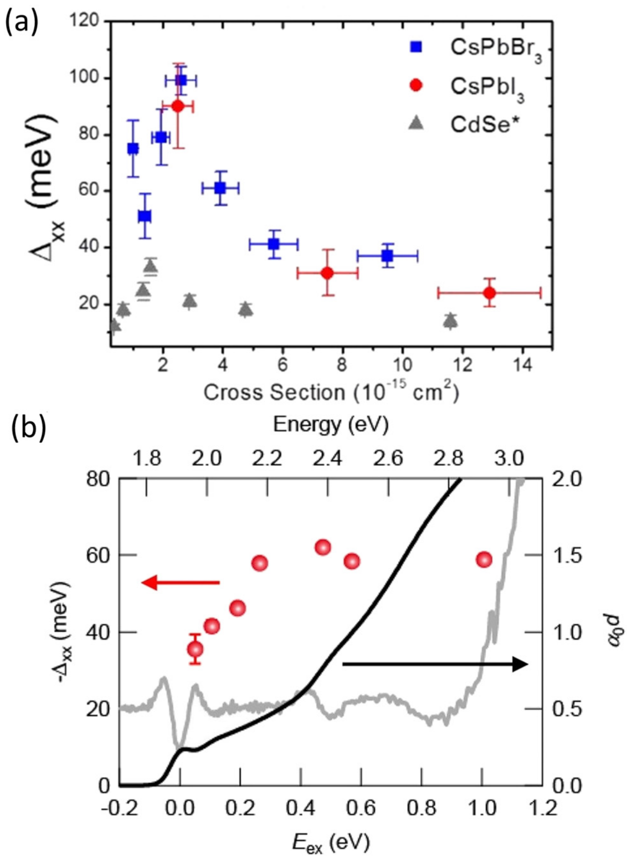

Figure 6: (a) Size dependence of biexciton binding energy of $CsPbBr_3$ and $CsPbI_3$ quantum dots [15]. (b) Estimated excess energy dependence of the biexciton binding energy (red dots) [74].

produced by the interaction between hot excitons and band-edge excitons [1]. The optical properties of low dimensional materials are usually dominated by excitons [52]. In perovskite materials, the exciton-exciton interaction is attractive. It is expected that at room temperature exciton is the dominant carrier species in the 2D perovskite. When perovskite acts as light-emitting applications, efficient radiative recombination is desirable [79, 80], which requires a large exciton binding energy, as the free charge carriers can be easily quenched by defects and thus lead to reduced quantum efficiency [81]. The large binding energy indicates that the biexciton is stable at room temperature, also shows the increase of biexciton lifetime.

5 Conclusions

In this review, biexciton dynamics processes summarize mainly from biexciton lifetime and biexciton binding energy. The biexciton lifetime and biexciton binding energy are both important parts of multiple excitons dynamics. A relatively long biexciton lifetime is beneficial to the application of lead halide perovskite in light-emitting devices and photovoltaic devices. High biexciton binding energy can evaluate the stability and the threshold, which is expected to reduce the stimulated emission of radiation. Further study of multibody dynamics will be a powerful tool to illustrate a more comprehensive mechanism of the exciton process. Hence, it can be conducive to lead halide perovskite materials application, accelerating the improvement of solar cells and light-emitting devices.

Author contribution: Gao W. was responsible for designing the writing framework and full-text writing. Bai Z., Qi Y., Wang Y., and Lv Z. were responsible for the literature search. Ding J. was responsible for the review of the full text.

Research funding: This work was supported by the National Science Foundation of China (No. 62005075). Hebei Science & Technology Research Project (QN2020182) and Hebei Natural Science Foundation (F2020202029) are acknowledged for partial financial support.

Conflict of interest statement: The authors declare that they have no conflict of interest.

References

[1] B. R. C. Vale, E. Socie, A. Burgos-Caminal, et al., “Exciton, biexciton, and hot exciton dynamics in $CsPbBr_3$ colloidal nanoplatelets,” *J. Phys. Chem. Lett.*, vol. 11, no. 2, pp. 387–394, 2020.

[2] A. Jha, H.-G. Duan, V. Tiwari, et al., “Direct observation of ultrafast exciton dissociation in lead iodide perovskite by 2D electronic spectroscopy,” *ACS Photonics*, vol. 5, no. 3, pp. 852–860, 2018.

[3] Md. S. Islam, B. Dey, Md. M. Rana, et al., “Temperature-induced localized exciton dynamics in mixed lead–tin based $CH_3NH_3Pb_{1-x}Sn_xI_3$ perovskite mate-rials,” *AIP Adv*, vol. 10, p. 065331, 2020.

[4] J. Chen, J. Wang, X. Xu, et al., “Efficient and bright white light-emitting diodes based on single-layer heterophase halide perovskites,” *Nat. Photonics*, vol. 15, no. 3, pp. 238–244, 2021.

[5] G. Xing, N. Mathews, S. S. Lim, et al., “Low-temperature solution-processed wavelength-tunable perovskites for lasing,” *Nat. Mater*, vol. 13, no. 5, pp. 476–480, 2014.

[6] S. Yakunin, L. Protesescu, F. Krieg, et al., “Low-threshold amplified spontaneous emission and lasing from colloidal nanocrystals of caesium lead halide perovskites,” *Nat. Commun.*, vol. 6, no. 1, pp. 1–9, 2015.

[7] G. Nedelcu, L. Protesescu, S. Yakunin, et al., “Fast ani on-exchange in highly luminescent nanocrystals of cesium lead halide perovskites ($CsPbX_3$, X = Cl, Br, I),” *Nat. Commun.*, vol. 15, no. 8, pp. 5635–5640, 2015.

[8] J. Werner, C.-H. Weng, A. Walter, et al., "Efficient mono lithic perovskite/silicon tandem solar cell with cell area >1 cm^2," *J. Phys. Chem. Lett*, vol. 7, no. 1, pp. 161–166, 2016.

[9] X. Li, Z. Xue, D. Luo, et al., "A stable lead halide perovskite nanocrystal protected by PMMA," *Sci. China Mater.*, vol. 61, no. 3, pp. 363–370, 2018.

[10] X. Ding, Y. Ren, Y. Wu, et al., "Sequential deposition method fabricating carbon-based fully-inorganic perovskite solar cells," *Sci. China Mater.*, vol. 61, no. 1, pp. 73–79, 2017.

[11] F. Li, J. Lu, Q. Zhang, et al., "Controlled fabrication, lasing behavior and excitonic recombination dynamics in single crystal $CH_3NH_3PbBr_3$ perovskite cuboids," *Sci. Bull*, vol. 64, no. 10, pp. 698–704, 2019.

[12] K. Dave, Z. Bao, S. Nakahara, et al., "Improvement in quantum yield by suppression of trions in room temperature synthesized $CsPbBr_3$ perovskite quantum dots for backlight displays," *Nanoscale*, vol. 12, no. 6, pp. 3820–3826, 2020.

[13] Y. Yang, M. Yang, Z. Li, et al., "Comparison of recombination dynamics in $CH_3NH_3PbBr_3$ and $CH_3NH_3PbI_3$ perovskite films: influence of exciton binding energy," *J. Phys. Chem. Lett*, vol. 6, no. 23, pp. 4688–4692, 2015.

[14] A. Manzi, Y. Tong, J. Feucht, et al., "Resonantly enhanced multiple exciton generation through be-low-band-gap multi-photon absorption in perovskite nanocrystals," *Nat. Commun.*, vol. 9, no. 1, p. 1518, 2018.

[15] J. A. Castañeda, G. Nagamine, E. Yassitepe, et al., "Efficient biexciton interaction in perovskite quantum dots under weak and strong confinement," *ACS Nano*, vol. 10, no. 9, pp. 8603–8609, 2016.

[16] K. E. Shulenberger, M. N. Ashner, S. K. Ha, et al., "Setting an upper bound to the biexciton binding energy in $CsPbBr_3$ perovskite nanocrystals," *J. Phys. Chem. Lett*, vol. 10, no. 18, pp. 5680–5686, 2019.

[17] S. A. Kulkarni, N. Yantara, K. S. Tan, et al., "Perovskite nanostructures: leveraging quantum effects to challenge optoelectronic limits," *Mater. Today*, vol. 33, pp. 122–140, 2020.

[18] D. Lin, L. Ma, W. Ni, et al., "Unveiling hot carrier relaxation and carrier transport mechanisms in quasi two-dimensional layered perovskites," *J. Mater. Chem. A*, vol. 8, no. 47, pp. 25402–25410, 2020.

[19] E. M. L. D. De Jong, G. Yamashita, L. Gomez, et al., "Multiexciton lifetime in all-inorganic $CsPbBr_3$ perovskite nanocrystals," *J. Phys. Chem. C*, vol. 121, no. 3, pp. 1941–1947, 2017.

[20] J. Reding, W. Zhang, and J. Allam, "Imaging excited-state dynamics in two-dimensional semiconductors with emerging ultrafast measurement techniques," *Acc. Mater. Res.*, vol. 2, no. 2, pp. 75–85, 2021.

[21] J. Lu, W. Chen, C. Zhou, et al., "Layer number dependent exciton dissociation and carrier recombination in 2D Ruddlesden–Popper halide perovskites," *J. Mater. Chem. C*, vol. 9, no. 28, pp. 8966–8974, 2021.

[22] P. Heremans, D. Cheyns, and B. P. Rand, "Strategies for increasing the efficiency of heterojunction organic solar cells: material selection and device architecture," *Acc. Chem. Res*, vol. 42, no. 11, pp. 1740–1747, 2009.

[23] M. Graetzel, R. A. J. Janssen, D. B. Mitzi, et al., "Materials Interface engineering for solution-processed photovoltaics," *Nature*, vol. 488, no. 7411, pp. 304–312, 2012.

[24] D. J. Vogel, A. Kryjevski, T. Inerbaev, et al., "Photoinduced single and multiple-electron dynamics processes enhanced by quantum confinement in lead halide perovskite quantum dots," *J. Phys. Chem. Lett*, vol. 8, no. 13, pp. 3032–3039, 2017.

[25] D. Giovanni, M. Righetto, Q. Zhang, et al., "Origins of the long-range exciton diffusion in perovskite nanocrystal films: photon recycling vs exciton hopping," *Light Sci. Appl*, vol. 10, no. 1, p. 2, 2021.

[26] N. Yarita, H. Tahara, T. Ihara, et al., "Dynamics of charged excitons and biexcitons in $CsPbBr_3$ perovskite nanocrystals revealed by femtosecond transient-absorption and single-dot luminescence spectroscopy," *J. Phys. Chem. Lett*, vol. 8, no. 7, pp. 1413–1418, 2017.

[27] H. He, "Lead halide perovskites: recombining faster, emit ting brighter," *Sci. China Mater.*, vol. 61, no. 8, pp. 1135–1136, 2018.

[28] X. Deng, X. Wen, S. Huang, et al., "Ultrafast carrier dynamics in methylammonium lead bromide perovskite," *J. Phys. Chem. C*, vol. 120, no. 5, pp. 2542–2547, 2016.

[29] H. Wang, L. Whittaker-Brooks, and G. R. Fleming, "Exciton and free charge dynamics of methylammonium lead iodide perovskites are different in the tetragonal and orthorhombic phases," *J. Phys. Chem. C*, vol. 119, no. 34, pp. 19590–19595, 2015.

[30] C. Sheng, C. Zhang, Y. Zhai, et al., "Exciton versus free carri er photogeneration in organometal trihalide perovskites probed by broadband ultrafast polarization memory dynamics," *Phys. Rev. Lett.*, vol. 114, no. 11, p. 116601, 2015.

[31] H.-H. Fang, L. Protesescu, D. M. Balazs, et al., "Exciton recombination in formamidinium lead triiodide: nanocrystals versus thin films," *Small*, vol. 13, no. 32, p. 1700673, 2017.

[32] D. A. Valverde-Chávez, C. S. Ponseca, C. C. Stoumpos, et al., "Intrinsic femtosecond charge generation dynamics in single crystal $CH_3NH_3PbI_3$," *Energy Environ. Sci.*, vol. 8, no. 12, pp. 3700–3707, 2015.

[33] P. Piatkowski, B. Cohen, C. S. Ponseca, et al., "Unravelling charge carriers generation, diffusion, and recombination in formamidinium lead triiodide perovskite polycrystalline thin film," *J. Phys. Chem. Lett*, vol. 7, no. 1, pp. 204–210, 2016.

[34] A. Marchioro, J. Teuscher, D. Friedrich, et al., "Unravelling the mechanism of photoinduced charge transfer processes in lead iodide perovskite solar cells," *Nat. Photonics*, vol. 8, no. 3, pp. 250–255, 2014.

[35] P. Piatkowski, B. Cohen, F. Javier Ramos, et al., "Direct monitoring of ultrafast electron and hole dynamics in perovskite solar cells," *Phys. Chem. Chem. Phys.*, vol. 17, no. 22, pp. 14674–14684, 2015.

[36] A. M. Soufiani, F. Huang, P. Reece, et al., "Polaronic exciton binding energy in iodide and bromide organ-ic-inorganic lead halide perovskites," *Appl. Phys. Lett.*, vol. 107, no. 23, p. 231902, 2015.

[37] J. Shi, Y. Li, J. Wu, et al., "Exciton character and high-performance stimulated emission of hybrid lead bromide perovskite polycrystalline film," *Adv. Opt. Mater.*, vol. 8, no. 10, p. 1902026, 2020.

[38] S. Ahmad, P. K. Kanaujia, H. J. Beeson, et al., "Strong photo current from two-dimensional excitons in solution-processed stacked perovskite semiconductor sheets," *ACS Appl. Mater. Interfaces*, vol. 7, no. 45, pp. 25227–25236, 2015.

[39] A. H. Proppe, M. H. Elkins, O. Voznyy, et al., "Spectrally resolved ultrafast exciton transfer in mixed perovskite quantum wells," *J. Phys. Chem. Lett*, vol. 10, no. 3, pp. 419–426, 2019.

[40] N. Sestu, M. Cadelano, V. Sarritzu, et al., “Absorption F-sum rule for the exciton binding energy in methylammonium lead halide perovskites,” *J. Phys. Chem. Lett*, vol. 6, no. 22, pp. 4566–4572, 2015.

[41] B. Luo, Y.-C. Pu, Y. Yang, et al., “Synthesis, optical properties, and exciton dynamics of organolead bromide perovskite nanocrystals,” *J. Phys. Chem. C*, vol. 119, no. 47, pp. 26672–26682, 2015.

[42] C. de. Weerd, L. Gomez, A. Capretti, et al., “Efficient carrier multiplication in $CsPbI_3$ perovskite nano-crystals,” *Nat. Commun.*, vol. 9, no. 1, pp. 1–9, 2018.

[43] N. Mondal, A. De, and A. Samanta, “All-inorganic perovskite nanocrystal assisted extraction of hot electrons and biexcitons from photoexcited CdTe quantum dots,” *Nanoscale*, vol. 10, no. 2, pp. 639–645, 2018.

[44] E. Kobiyama, H. Tahara, R. Sato, et al., “Reduction of optical gain threshold in $CsPbI_3$ nanocrystals achieved by generation of asymmetric hot-biexcitons,” *Nano Lett*, vol. 20, no. 5, pp. 3905–3910, 2020.

[45] R. A. Lazo, R. Saran, O. Woolland, et al., “Exciton effects in perovskite nanocrystals,” *J. Phys.: Photonics*, 2021. https://doi.org/10.1088/2515-7647/abedd0.

[46] M. Li, R. Begum, J. Fu, et al., “Low threshold and efficient multiple exciton generation in halide perovskite nanocrystals,” *Nat. Commun.*, vol. 9, no. 1, pp. 1–7, 2018.

[47] J. Aneesh, A. Swarnkar, V. Kumar Ravi, et al., “Ultrafast exciton dynamics in colloidal $CsPbBr_3$ perovskite nanocrystals: biexciton effect and auger recombination,” *J. Phys. Chem. C*, vol. 121, no. 8, pp. 4734–4739, 2017.

[48] C. de. Weerd, L. Gomez, A. Capretti, et al., “Efficient carrier multiplication in $CsPbI_3$ perovskite nanocrystals,” *Nat. Commun.*, vol. 9, no. 1, pp. 1–9, 2018.

[49] C. Weerd, “Efficient carrier multi plication in $CsPbI_3$ perovskite nanocrystals,” *Nat. Commun.*, p. 9, 2018. https://doi.org/10.1038/s41467-018-06721-0.

[50] H. Eshet, R. Baer, D. Neuhauser, et al., “Theory of highly efficient multiexciton generation in type-II nanorods,” *Nat. Commun.*, vol. 7, no. 1, p. 13178, 2016.

[51] M. T. Trinh, X. Wu, D. Niesner, et al., “Many-body in ter-actions in photo-excited lead iodide perovskite,” *J. Mater. Chem. A*, vol. 3, no. 17, pp. 9285–9290, 2015.

[52] H.-H. Fang, J. Yang, S. Adjokatse, et al., “Band-edge exciton fine structure and exciton recombination dynamics in single crystals of layered hybrid perovskites,” *Adv. Funct. Mater*, vol. 30, no. 6, p. 1907979, 2020.

[53] A. Shukla, G. Kaur, K. J. Babu, et al., “Effect of confinement on the exciton and biexciton dynamics in perovskite 2D-nanosheets and 3D-nanocrystals,” *J. Phys. Chem. Lett.*, vol. 11, no. 15, pp. 6344–6352, 2020.

[54] F. Thouin, “Stable biexcitons in two-dimensional metal-halide perovskites with strong dynamic lattice disorder,” *Phys. Rev. Mater.*, vol. 2, no. 3, 2018. https://doi.org/10.1103/physrevmaterials.2.034001.

[55] Y. Kanemitsu, “Trion dynamics in lead halide perovskite nanocrystals,” *J. Chem. Phys*, vol. 151, no. 17, p. 170902, 2019.

[56] Y. Wang, X. Li, J. Song, et al., “All-inorganic colloidal perovskite quantum dots: a new class of lasing materials with favourable characteristics,” *Adv. Mater.*, vol. 27, no. 44, pp. 7101–7108, 2015.

[57] N. Mondal, A. De, and A. Samanta, “Biexciton generation and dissociation dynamics in formamidinium and chloride-doped cesium lead iodide perovskite nanocrystals,” *J. Phys. Chem. Lett.*, vol. 9, no. 13, pp. 3673–3679, 2018.

[58] V. I. Klimov, “Optical nonlinearities and ultrafast carrier dynamics in semiconductor nanocrystals,” *J. Phys. Chem. B*, vol. 104, no. 26, pp. 6112–6123, 2000.

[59] N. S. Makarov, S. Guo, O. Isaienko, et al., “Spectral and dynamical properties of single excitons, biexcitons, and trions in cesium–lead-halide perovskite quantum dots,” *Nano Lett*, vol. 16, no. 4, pp. 2349–2362, 2016.

[60] J. Li, Q. Jing, S. Xiao, et al., “Spectral dynamics and multiphoton absorption properties of all-inorganic perovskite nanorods,” *J. Phys. Chem. Lett.*, vol. 11, no. 12, pp. 4817–4825, 2020.

[61] K. Wu, G. Liang, Q. Shang, et al., “Ultrafast interfacial electron and hole transfer from $CsPbBr_3$ perovskite quantum dots,” *J. Am. Chem. Soc*, vol. 137, no. 40, pp. 12792–12795, 2015.

[62] H. Zhu, Y. Fu, F. Meng, et al., “Lead halide perovskite nanowire lasers with low lasing thresholds and high quality factors,” *Nat. Mater.*, vol. 14, no. 6, pp. 636–642, 2015.

[63] L. Protesescu, S. Yakunin, M. I. Bodnarchuk, et al., “Nanocrystals of cesium lead halide perovskites ($CsPbX_3$, X = Cl, Br, and I): novel optoelectronic materials showing bright emission with wide color gamut,” *Nano Lett.*, vol. 15, no. 6, pp. 3692–3696, 2015.

[64] K. Galkowski, A. Mitioglu, A. Miyata, et al., “Determination of the exciton binding energy and effective masses for methylammonium and formamidinium lead tri-halide perovskite semiconductors,” *Energy Environ. Sci.*, vol. 9, no. 3, pp. 962–970, 2016.

[65] P. Tyagi, S. M. Arveson, and W. A. Tisdale, “Colloidal organohalide perovskite nanoplatelets exhibiting quantum confinement,” *J. Phys. Chem. Lett.*, vol. 6, no. 10, pp. 1911–1916, 2015.

[66] J. Li, L. Luo, H. Huang, et al., “2D behaviors of excitons in cesium lead halide perovskite nanoplatelets,” *J. Phys. Chem. Lett.*, vol. 8, no. 6, pp. 1161–1168, 2017.

[67] M. Yu, S. Yuan, H.-Y. Wang, et al., “Characterization of the influences of morphology on the intrinsic properties of perovskite films by temperature-dependent and time-resolved spectroscopies,” *Phys. Chem. Chem. Phys.*, vol. 20, no. 9, pp. 6575–6581, 2018.

[68] B. Cheng, T.-Y. Li, P. Maity, et al., “Extremely reduced dielectric confinement in two-dimensional hybrid perovskites with large polar organics,” *Commun. Phys*, vol. 1, no. 1, pp. 1–8, 2018.

[69] K. Tanaka and T. Kondo, “Bandgap and exciton binding energies in lead-iodide-based natural quantum-well crystals,” *Sci. Technol. Adv. Mater.*, vol. 4, no. 6, pp. 599–604, 2003.

[70] J. Cho, J. T. DuBose, and P. V. Kamat, “Charge carrier Re combination dynamics of two-dimensional lead halide perovskites,” *J. Phys. Chem. Lett.*, vol. 11, no. 7, pp. 2570–2576, 2020.

[71] J.-C. Blancon, A. V. Stier, H. Tsai, et al., “Scaling law for excitons in 2D perovskite quantum wells,” *Nat. Commun.*, vol. 9, no. 1, p. 2254, 2018.

[72] J. Nanda, S. A. Ivanov, M. Achermann, et al., “Light amplification in the single-exciton regime using Exciton–Exciton repulsion in type-II nanocrystal quantum dots,” *J. Phys. Chem. C*, vol. 111, no. 42, pp. 15382–15390, 2007.

[73] Y. Kato, D. Ichii, K. Ohashi, et al., “Extremely large binding energy of biexcitons in an organic–inorganic quantum-well material $(C_4H_9NH_3)_2PbBr_4$,” *Solid State Commun*, vol. 128, no. 1, pp. 15–18, 2003.

[74] G. Yumoto, H. Tahara, T. Kawawaki, et al., "Hot biexciton effect on optical gain in $CsPbI_3$ perovskite nanocrystals," *J. Phys. Chem. Lett.*, vol. 9, no. 9, pp. 2222–2228, 2018.

[75] M. N. Ashner, K. E. Shulenberger, F. Krieg, et al., "Size-dependent biexciton spectrum in CsPbBr3 perovskite nanocrystals," *ACS Energy Lett.*, 2019. https://doi.org/10.1021/acsenergylett.9b02041.

[76] M. Nirmal and L. Brus, "Luminescence photophysics in semiconductor nano crystals," *Acc. Chem. Res*, vol. 32, no. 5, pp. 407–414, 1999.

[77] T. Fujita, Y. Sato, T. Kuitani, et al., "Tunable polariton absorption of distributed feedback microcavities at room temperature," *Phys. Rev. B*, vol. 57, no. 19, pp. 12428–12434, 1998.

[78] X. Hong, T. Ishihara, and A. V. Nurmikko, "Dielectric confinement effect on excitons in PbI_4-based layered semiconductors," *Phys. Rev. B*, vol. 45, no. 12, pp. 6961–6964, 1992.

[79] M. Yuan, L. N. Quan, R. Comin, et al., "Perovskite energy funnels for efficient light-emitting diodes," *Nat. Nanotechnol*, vol. 11, no. 10, pp. 872–877, 2016.

[80] G. Xing, B. Wu, X. Wu, et al., "Transcending the slow bimolecular recombination in lead-halide perovskites for electroluminescence," *Nat. Commun*, vol. 8, no. 1, pp. 1–9, 2017.

[81] J. Lu, W. Chen, C. Zhou, et al., "Layer number dependent exciton dissociation and carrier recombination in 2D Ruddlesden–Popper halide perovskites," *J. Mater. Chem. C*, vol. 9, no. 28, pp. 8966–8974, 2021.